Improvement of Applicability of Snow Hydrological Model by Introducing Snow Correction Factor in the Gilgit Basin

Cheema, S. B.[1, 2], M. Afzaal[2], T. Koike[3], M. Rasmy[3]

Abstract

In order to estimate spatial and temporal distribution of snow cover and associated discharge in Gilgit basin, a physical based snow hydrological model (WEB-DHM-S) version 0.9.7 was developed for study area. The influence of several forcing data against snow thawing and freezing process investigated and correction method was developed for these data sets. The simulated results were assessed by introducing renowned efficiency tests such as Nash Sutcliffe Efficiency (NSE), Relative Volume Error (RVE) and Root Mean Square Error (RMSE). A grid to grid comparison was also made using Kuipers Skill Score and False Alarm Rate (FAR) by two contingency table. The deficiency of Japan Reanalysis-55 (JRA) gridded temperature data was overcome by introducing observed data with adjustment of temperature lapse rate for each model grid. Most of the rainfall gauges were located at lower latitude of the basin except Yasin station. Precipitation was corrected with respect to elevation by considering the fact that high elevation experiences more precipitation and snowfall. Even though precipitation correction provided better results, but simulated snowmelt process was still delayed. This issue was solved by changing fresh snow albedo from 0.90 to 0.80, resulting good correlation with observed data and justify by statistical analysis. The model was developed only for snow dynamics but glacier contribution is necessary for accurate discharge.

Keywords: Temperature; Lapse Rate; Precipitation Correction Factor; Gilgit River Basin; Simulated; snow dynamics

Introduction

Pakistan is a home of more than 5000 snow reservoir and glaciers along with the second largest Siachen glacier (Rasul et al., 2011). The fresh water is preserved in these reservoir during the winter season and feed to the river in the summer season due to the gradual melting of ice and snow in upper parts of the country.

The Indus River run off is highly depends upon snow melt in these upper parts. More than 70% cultivated area lies along the Indus River (Thenkabail et al., 2005).Being an agrarian country economy of Pakistan is directly related with the water availability of Indus. Major tributaries of Upper Indus Basin (UIB) are Shyok, Gilgit, Hunza and Astore River (Immerzeel et al., 2010). Sumer runoff is highly correlated with winter snow pack for Gilgit Basin as compared to all other basins (Tahir et al., 2010). Pakistan has limited resources for monitoring of snowfall and snow cover. There is no accurate tool or methods to measure snow cover or snowfall at high altitude. Snowfall measurement methods are very old and have many flaws in measurement. The snow depth measured with scale which caused lack of reliable data for research purpose. Many diverse approaches have been taken in developing hydrological models for better representation of snow processes, ranging from simplified temperature index models to physically based single or multi-layer energy-balance snowmelt models (Shrestha et al., 2010). Marks reported in his study that energy exchange method is much better than temperature degree day method to calculate snowmelt (Marks et al., 1992). Almost 70 % area of Gilgit basin is covered with snow which was calculated from Digital Elevation Model (DEM) data in this study. The Gilgit River incorporate the Yasin, Hunza and Ishkuman River (Bashir & Rasul, 2010). The Gilgit River originate from Shindoor river and one of the major tribute of Indus river, before Gilgit and Skardu the Indus river is like a stream, when Indus enter in Pakistan it receive large amount of snow and glaciated water.

[1] Sohailbabar.cheema@gmail.com
[2] Pakistan Meteorological Department, Pitras Bukhari Road, Sector H-8/2, Islamabad, Pakistan.
[3] ICHARM, Public Works Research Institute, Japan.

The basin area is significantly covered with snow as compared to all other basin of UIB as shown in Figure 1. The total calculated watershed area is 16513.139 km^2 out of which snow covered area is 68.74 percent. Above 5500 m elevation the land area is covered with permafrost that is 13.4% of total area of the water shed. As discussed before a large chunk is snow covered, so the flow of the Gilgit River is highly depends upon snowfall. Moreover the perpetual discharge varies from winter to summer. The average annual discharge was 600.2745 m^3/sec. The highest discharge was observed in July that is more than 2000 m^3/sec.

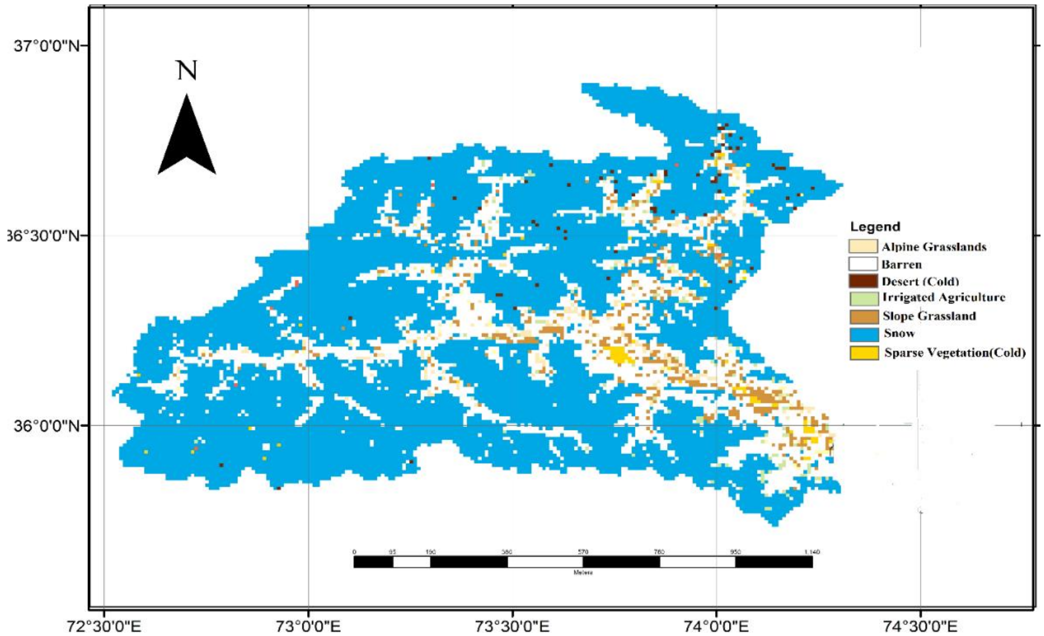

Figure 1: Land covered area of Gilgit

The main cause of this high discharge is due to snow melting. After the month of September discharge starts to decrease.

Table 1: Gilgit River Basin characteristics

Gilgit River Basin	
Total Watershed Area	16722.75 km^2
Snow Cover Area	68.74 %
Glacier Cover Area	13.4%
Mean Elevation	1400-6000 (meter)
Annual Average Discharge	600.28m^3/sec

This paper presents the three different approaches in order to improve the applicability of energy based hydrological model (WEB-DHM; Wang et al., 2009a, b) for the simulations of the snow process and related discharge. Initially observed temperature data feed directly instead of JRA-55 data then lapse rate is applied for that temperature. Next an equation was developed for enhancing precipitation with respect to altitude. After applying the proposed equation model was evaluated by different statistical test both for snow accumulation and discharge.

Data and Methodology

Static and dynamic data sets were used in this study. The static data includes land use data, topographic data of Digital Elevation Model (DEM), Soil data etc. These data were processed at a resolution of 500 meter. In dynamic data, forcing data like wind, relative or specific humidity, cloud cover, air pressure, short wave and long wave incoming solar radiation were used. These forcing data were three hourly, six hourly, daily and monthly mean variance data with a resolution of 0.5625˚ (60 km). The data were downloaded from URL https://rda.ucar.edu/datasets/ds628.0_and extracted for study area. The Japan Meteorological Agency (JMA) started the second global atmospheric reanalysis project named the Japanese-55-year Reanalysis (JRA-55). There are many deficiencies found in the first version of Japanese reanalysis data set (JRA-25), after that the Japanese 25-year Reanalysis (JRA-25) have been improved. Its purpose was to provide a comprehensive dataset that is suitable for study of climate change or multi-decadal variability, by producing a more time consistent data set for longer time than 25 year. Production of JRA-55 was completed in 2013 and after that it was continued as a new JMA Climate Data Assimilation System (JCDAS) on real time basis (Ayataka et al., 2011). Model grid size was 500 m, so all these forcing data sets were interpolated or resampled to this spatial resolution. The vegetation forcing data Leaf Area Index (LAI) were downloaded (http://reverb.echo.nasa.gov /).

Model Structure

The overall structure of WEB-DHM, and the sub grid parameterization as well as detailed description of the vertical 3 layered energy balance is shown in Figure 2 and can be explained as:

- The target basin is divided into sub basin by using a digital elevation model for 450 m horizontal resolution, target area was defined at predefined grid size (500 m in this research).
- The main streams located in a flow interval are agglutinated into a single virtual channel of trapezoid shape and lead to the outlet of the basin as shown in Figure 2 (a).

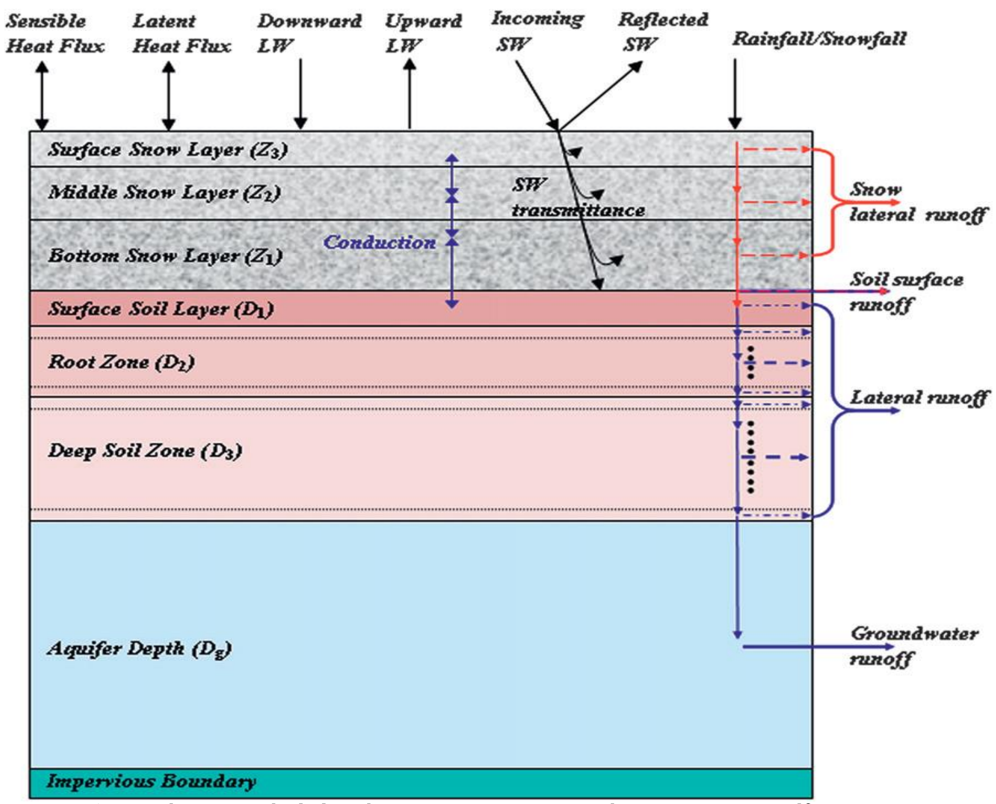

(Source: http://www.hydrol-earth-syst-sci.net/14/2577/2010/hess-14-2577-2010.pdf)

Figure 2: Overall structures of WEB-DHM and WEB-DHM-S

- The length and slope for each grid value is extracted by processing of DEM data as shown in Fig 2 (b). For simplicity it is considered that a large grid comprises a set of small symmetrical hill slopes situated along the streams. The length of a hill slope is calculated as

  Length = A/2 ∑ L

  A = total area of river

L = Total length of stream

The grid slope is taken as the average of all sub grid slope in the DEM data (Tarboton, 1997).

- As stated previously the main river is divided into river network by the code of the divided sub basin (Verdin et.al, 1999).

Snow Process in WEB-DHM and WEB-DHM-S

The snow parameterization for sub model in WEB-DHM is same as for SiB2 scheme (Sellers et al., 1996). In case of large snow mass only the upper surface of snow up to 05 cm of snow water equivalent (SWE) is derived as a variation of the heat capacity for surface skin that affects the surface energy balance. Albedo ratio for dry snow is kept at a constant value of 0.4 for near infrared (NIR) short wave radiation and 0.8 for visible shortwave radiation. The albedo ratio is set to be 60% for dry snow and temperature of snow is consider to be equivalent to the ground temperature. Snow surface temperature, that is drive as an average snow pack temperature tends to results in an incorrect simulation of the surface energy budget which in turn affect the overall accumulation and melting process (M Shrestha, Wang, Koike, Xue, & Hirabayashi, 2010).

In the new version of WEB-DHM the snow physics was improved by Shrestha and rename it as WEB-DHM-S, in this new version the single layer of snow that is more than 05 cm is distributed into main three layers with varying depth and snow density. There is 02 cm thickness for the top layer of snow and 20 cm for the middle layer and the snow depth for remaining part is considered third layer as shown in Figure 3.1 (b). But the snow parameterization for the canopy is same as for WEB-DHM, however this time snow albedo scheme is parameterized by using another scheme known as Bio-sphere Atmospheric Transfer Scheme (BATS) (Dickinson, Henderson-Sellers, & Kennedy, 1993). In short the mass budget for each layer is found by calculating the evaporation, precipitation, liquid water confinement, infiltration in each layer and snow melt run off for accumulated snow.

Temperature Lapse Rate and Precipitation Correction Factor for Model Development

The Gilgit Basin is covered by MODIS scan of MOD10A2h23v05 and MODIS10A2h24v05, with 500-meter resolution. Observed rainfall and temperature data were obtained from Pakistan Meteorological Department (PMD) and Water and Power Development Authority (WAPDA). The gridded temperature data has coarse resolution and cannot provide realistic distribution of snow cover, therefore, observed data were imported to the model in this study. The climate of Gilgit is moist most of the time during the year (Sandrine et al., 2006). Therefore a moist adiabatic lapse rate of 7.5˚C/km was used in this research .The temperature data were extrapolated to each model grid based on its elevation. The temperature lapse rate equation is as follows

$$T(i,j) = T_o - \{7.5 \times (Z(i,j) - h)/1000\} \tag{1}$$

Where T(i,j) is temperature at specific altitude, T_0 observed temperature for Gilgit observatory, z(i,j) elevation for all grids above than 1000 meter.

There was a very weak correlation between precipitation and elevation. Therefore in order to compensate precipitation at high elevation, the precipitation correction factor was used with the hypothesis that precipitation increased at high altitude. We applied following equation with different factors (values).

$$P_{h(i,j)} = P_o \times \{1 + \big(Z(i,j) - 1000\big) \times P_{cf}\} \tag{2}$$

Where i,j are latitude and longitude for each grid above than 1000 m.a.s.l, Z (i.j) is the two dimensional elevation, P_{cf} is a precipitation coefficient factor and P_0 observed precipitation (mm/hrs.). In this equation value of P_{cf} varies from 0.0005 to 0.001 for better improvement for discharge and snow cover area. The model performance was evaluated by using observed discharge data and 08 days composite Moderate Resolution Imaging Spectroradiometer (MODIS) data.

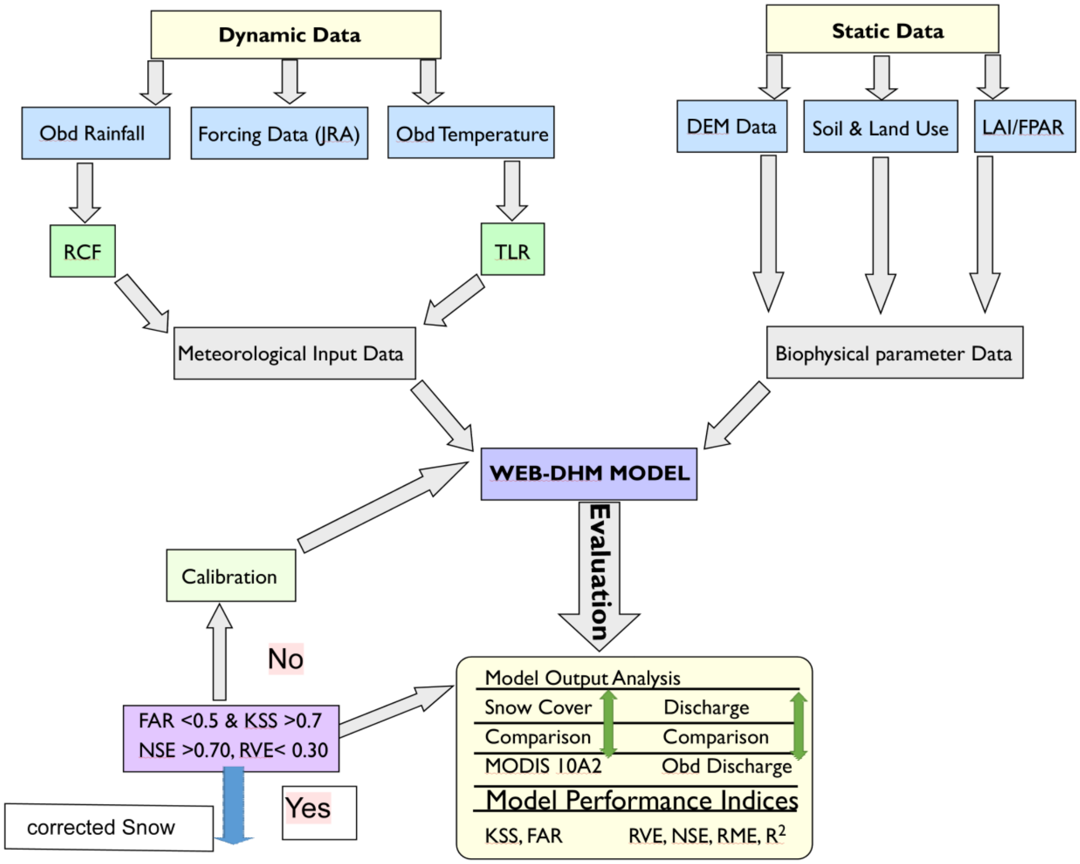

Figure 3: Methodology for Study

For this purpose different indices were used to confirm the improvement in the applicability of model against each factor. The flow chart diagram methodology is shown in Figure 3.

Results and Discussions

First of all the simulations were performed for gridded JRA temperature and rainfall data. The simulated snow cover area was not distributed in reliable manner. The whole basin was divided into two patches snow or no snow as shown in Figure 4(a). This was because of coarse resolution of temperature gridded

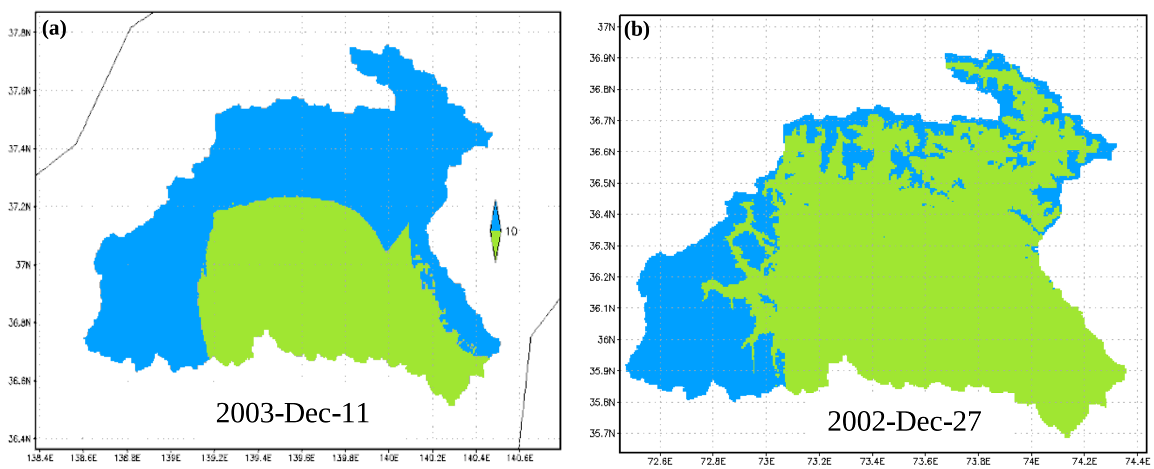

Figure 4: Simulated snow cover area. The blue region is snow and white one is land cover area.

data and high complex region of Gilgit. The observed temperature was imported after changing the source code and rainfall data by applying zero elevation method. The same method was earlier used by Shresta in his study (Shrestha et al., 2012). After this correction the snow distribution was synchronized with MODIS imaginary, although the simulation was still underestimated as shown in Figure 4 (b).

Rainfall and Elevation Relationship

Wang et al.,(2009) reported that south west Himalaya was influenced by the annual precipitation ranging from 150 mm to 500 mm at altitude of 1500-3000 m.a.s.l, whereas more than 1700 mm at an altitude of 5500 m.a.s.l. A weak correlation was found between altitude and daily rainfall for four years (2002-2005) data sets. The calculated correlation co-efficient was only 0.003 which mean there was a poor correlation between these above mentioned variables (rainfall and altitude). So, different attempts were made to enhance precipitation (rainfall and snow). In first attempt rainfall was increased by 1.5 times but the simulated results of discharge and snow cover was not well correlated with observed discharge and MODIS snow cover. The Kupier Skill Score (KSS) and False alarm Rate (FAR) was less than their absolute value which is 1 for KSS and 0.0 for FAR which shows that simulated results are not well synchronized with MODIS snow cover (Table 4).

Precipitation Correction Factor

The relationship between altitude (z) and hourly snowfall is given in equation 2. First of all simulation for P_{cf} 0.0005 was performed, then P_{cf} 0.0007 and P_{cf} 0.001respectively.The simulated discharge was analyzed for temperature lapse rate and each snowfall correction factor by using different statistical indices like Nash Sutcliff Efficiency (NSE), Root Mean Square Error (RMSE), Degree Index –d Relative Volume Error (RVE), Percentage Bias

(PBIAS) and coefficient of determination R^2. The performance for each factor is shown in Table 2 and discharge against each factor is represented in Figure 5(a-d). The Pcf is defined in equation 02 for precipitation at different grid levels.

Table 2: Efficiency test for discharge comparison between observed and simulated

Efficiency test	TLR	RCF	Pcf (0.0005)	Pcf (0.0007)	Albedo	Pcf+Albedo (0.001)
NSE	-0.09	1.5	0.46	0.53	0.64	0.72
r	0.52	0.20	0.75	0.76	0.80	0.86
RMSE	633.03	0.67	445.76	427.91	357.00	312.00
R^2	0.27	543.65	0.58	0.62	0.77	0.84
Index-d	0.44	0.44	0.78	0.79	0.82	0.88
RVE	-0.68	0.60	-0.43	-0.36	-0.32	-0.15
PBIAS	-68.44	-0.56	-43.36	-36.21	-32.12	-21.41

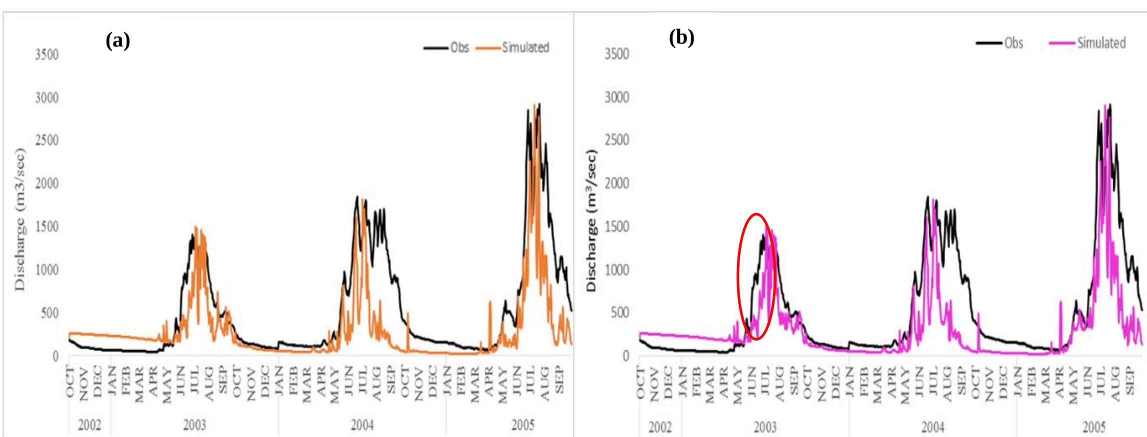

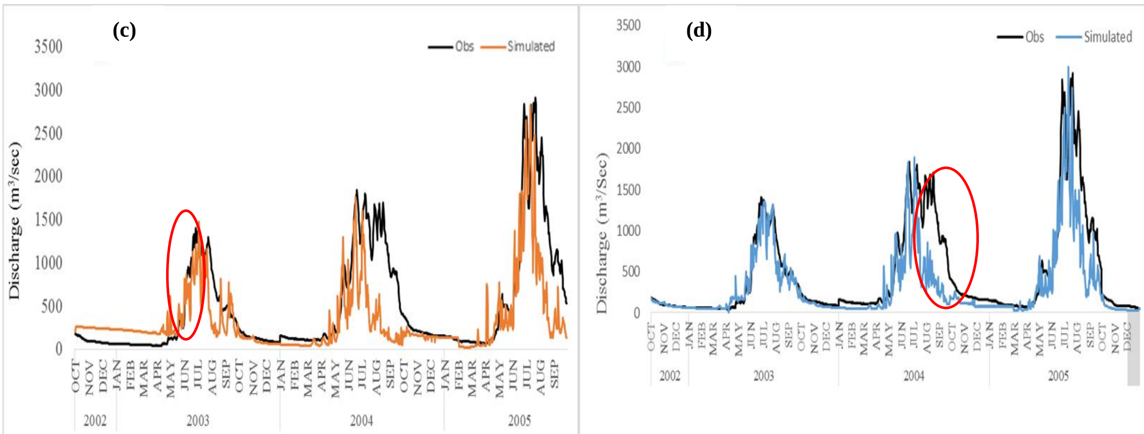

Figure 5: (a-d) A Comparisons between observed and simulated discharge (Oct, 2002-Sep, 2005). **(a)** For Pcf 0.0005 **(b)** for Pcf 0.0007, **(c)** for albedo 0.80 **(d)** for Pcf 0.001 and albedo 0.80.

The Figure 5 (a) portrays discharge comparison for Pcf 0.0005, 5(b) for Pcf 0.0007, 5(c) for albedo 0.80 and Figure 5 (d) represents for Pcf 0.001 and albedo 0.80. The value of precipitation correction factor was calculated from equation 2. According to above equation 02 PCF = R/1000. Where R stands for rainfall. The values of R are explained in below table 03.

Table 3: PCF and Albedo factors

S/No	R Value	PCF	Albedo Value
1	0.5	0.0005	90%
2	0.7	0.0007	90%
3	1	0.001	80%

It is worth mentioning here that in the simulations rainfall, temperature and precipitation was incorporated as depicted in Figure 5(a). After applying precipitation factor with value 0.0007, simulated discharge was enhanced but the change was not significant as shown in figure 5(b). The discharge was highly underestimated during June, July. This underestimation is due to no proper snow melting during this season. In all previous simulation default albedo value of 0.90 was used, but albedo change according to grain size and shape of snowflakes. Thus model was also tuned by adjusting albedo 0.80 instead of 0.90. In June, July snow grains are larger as compared to January and February (wang et_al., 2009). Therefore, albedo parameter was calibrated for albedo 0.80. The output simulated result shown in Figure 5(C). But, the values for proposed indices were not significant after apply factor 0.0007. Thus the precipitation was increased by a new factor 0.001for all those grids above than 1000 m.a.s.l as described in equation 3. A low increase in discharge start from start of May, since snowpack start melting in May and this discharge got its maximum peak in July-August due to large intensification of solar radiation. The simulated hydrograph coincide well with the observed hydrograph from accumulation to ablation period. Now the model capture the seasonal variation well which was due to sufficient precipitation and more energy budget provided for accumulation and melting as shown in Figure 5(d).

$$P_{h(Gilgit)} = P_h\ (1+(elev_{2d}(I,j)-1000)\ X\ 1.0/1000) \qquad (3)$$

Simulated discharge was well replicated with observed discharge; furthermore it was still underestimated for peak discharge. The maximum difference was observed in 2004. It was compulsory to investigate the cause for this underestimation of simulated discharge. The cause for this underestimation was verified in Figure 6.

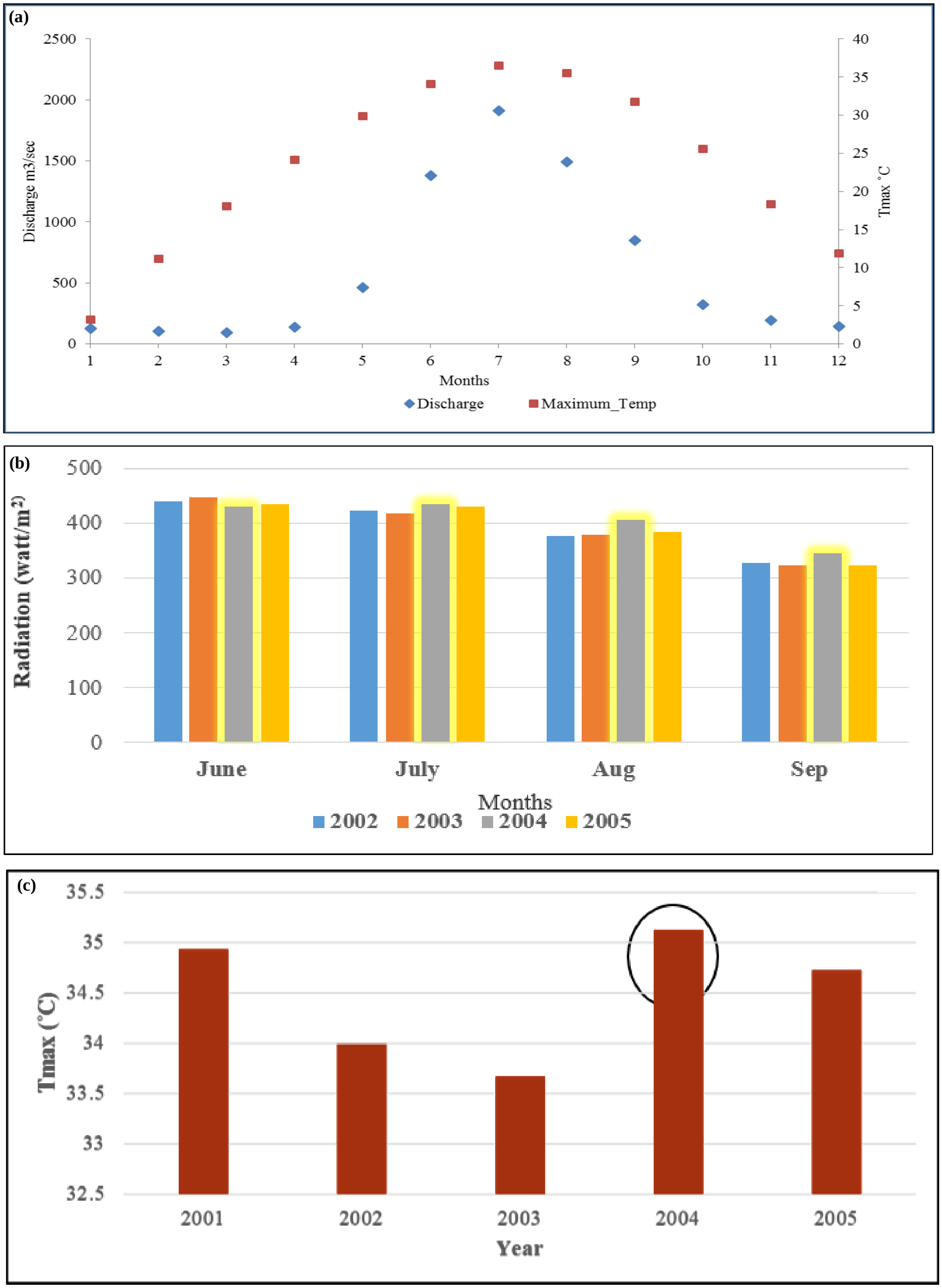

Figure 6: (a) Monthly comparison (2001-2005) between Tmax and observed discharge, **(b)** Short wave radiation **(c)** Maximum Temperature (˚C) for June to September for study period

The Figure 6 (a) is a monthly comparison between maximum temperatures (˚C) and observed discharge. Figure 6 (b) represents monthly mean value of incoming short wave radiations. These shortwave radiations play an important role in snow melting process. The picture 6 (b) clearly shows that during 2004 intensity of short wave was maximum during summer season as compared to all other years of study period (2002-2005). Similarly Figure 6 (C) represents the monthly average value for maximum temperature for Gilgit Basin during summer season. The maximum temperature was observed in 2004, which was above than 35°C. Therefore, it is pertinent to mention here this high temperature caused rapid melting process in these months.

Model was incorporated only for snow dynamics; therefore maximum difference in discharge during 2004 was due to glaciated region. This glaciated region is above 5500 m.a.sl. in Gilgit which was calculated from land cover area. So, thawing process of active permafrost at high elevation should be incorporated in new version of WEB-DHM-S.

A grid to grid analysis for different season was done by two contingency table and results are shown in Table 4 for each precipitation factor. The KSS indices values improved upto significant level and similarly value of FAR indices also decreased. After introducing Pcf 0.001, FAR was less than 45 that was acceptable. A grid to grid comparison between MODIS and simulated shows that model predict snow cover area in a well manner for peak season but in other seasons it was not good as compared to Feb-Apr seasons. But the KSS indices more than 0.70 and FAR less than 0.45 in these seasons.

MODIS and Model Snow Cover Area Comparison

The simulated results were processed in Grid Analysis and Data Display System (GrADS) for comparison with MODIS imaginary. The spatial distribution areal extent of snow cover area derived from model simulation and MODIS snow products for different seasons are presented in Figure 7. The Figure 7 represents that the correction factors are helpful in improvement for model applicability for a complex topographical region like Gilgit. The model is able to predict a small SCA after calibration with fresh snow albedo 0.80 and Pcf 0.001 untill end of November at high altitude with significant value of KSS that was greater than 0.70 for all the months of the year. The KSS indicates that trend of mid season ablation between January and March is found to be highly correlated with MODIS products. The FAR index also was below than 0.25 for February to April as shown in Table 4.

Table 4: Comparisons of snow cover area between MODIS and simulated for different precipitation factor.

	Oct-Dec		Feb-Apr		Jul-Sep	
Indices	KSS	FAR	KSS	FAR	KSS	FAR
TLR	0.41	0.74	0.52	0.53	-0.08	0.81
RCF1.5	0.47	0.62	0.64	0.49	0.02	0.77
PCF(0.0005)	0.6	0.57	0.76	0.46	0.32	0.66
PCF(0.0007)	0.66	0.52	0.84	0.37	0.55	0.54
PCF(0.001)	0.77	0.41	0.91	0.23	0.74	0.42

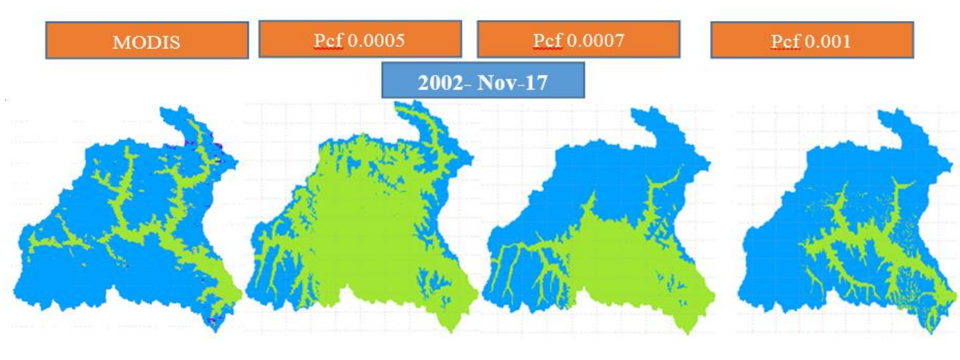

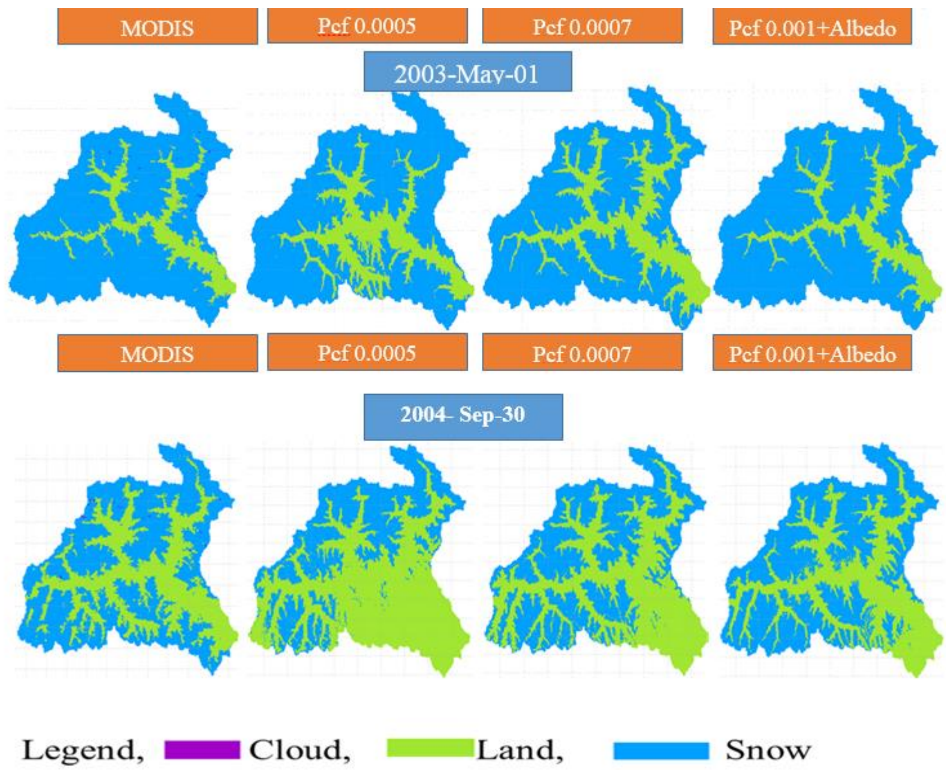

Figure 7: A spatial distribution comparisons of simulated and MODIS snow cover area for different season.

Hence a grid to grid analysis shows simulation for snow is reasonably well, for optimized Pcf 0.001 the snow depth increased by 69 % of that calculated without Pcf correction factor. These analysis was done for different season like snow accumulation, snow ablation etc. Thus precipitation factors and observed temperature after applying lapse rate increased the applicability of model both for snow cover and discharge. In the depletion period model output result follows MODIS SCA except for a remarkable overestimation in May. On average the performance of the model is satisfactory with a coefficient of correlation of 89 % and bias of 18 %.

Recommendations

The future scope of this study is to expand the applicability of model for other basins for number of years to sketch a good picture of simulated snow and discharge. The correction factor approach can be used for forecasting summer run off in snow fed river. The simulated discharge was still underestimating in July, August and September; therefore glacier dynamics should be added in new version of Web-DHM-S 0.97 as it was not addressed in the current version. Regarding the issues of model validation, the uncertainty in the MODIS snow mapping algorithm should be analyzed in detail for cloud cover area. The satellite product should be used after cloud filtration or other satellite products like Landsat and ASTER should be used for further validation. Further research must be commenced for evaluating the applicability of the approach presented here to other regions.

Acknowledgement

I would like to express my gratitude to Japan International Cooperation Agency and Pakistan Meteorological Department to provide me such an opportunity. I would like to express my sincerest thanks to all the staff of International Center for Water Hazard and Risk Management, Tsukuba Japan for their guidance throughout my research work.

References

Annette, W., 2009: Literature study on the correction of precipitation measurements. FutMon C1-Met-29 (BY), Bavarian State Institute of Forestry, Freising, Germany.

Bashir, F., and G. Rasul, 2010: Estimation of Water Discharge from Gilgit Basin, using Remote Sensing, GIS and Runoff Modeling." Pakistan Journal of Meteorology 6.12: 97-113.

Bony, Sandrine, et al, (2006): How well do we understand and evaluate climate change feedback processes? *Journal of Climate* 19.15 (2006): 3445-3482.

Dickinson, R .E. Henderson-Sellers and P.J. Kennedy.(1993: Biosphere-Atmosphere Transfer Scheme Version 1e as Coupled to the NCAR Community Climate Model. NCAR Tech: Note 387+ STR, 77pp.

Ebita, A., S. Kobayashi, Y. Ota, M. Moriya, R. Kumabe, K. Onogi, Y. Harada, S. Yasui, K. Miyaoka, K. Takahashi, H. Kamahori, C. Kobayashi, H. Endo, M. Soma, Y. Oikawa, and T. Ishimizu, 2011: The Japanese 55-year Reanalysis "JRA-55": an interim report, SOLA, 7, 149-152, doi:10.2151/sola.2011-038.

Immerzeel, W. W., et al 2010: Satellite Derived Snow and Runoff Dynamics in the Upper Indus River Basin." Grazer Schriften der Geographie und Raumforschung 45 (2010): 303-312.

Lei, W., T. Koike,Y. Kun, Yeh, P. J .Feng, 2009: Assessment of a distributed biosphere hydrological model against streamflow and MODIS land surface temperature in the upper Tone River Basin. Journal of Hydrology, 377(1), 21-34.

Marks, Danny, Dozier, Jeff, Davis and E .Robert, 1992: Climate and energy exchange at the snow surface in the alpine region of the Sierra Nevada: 1. Meteorological measurements and monitoring. Water Resources Research, 28(11), 3029-3042.

Rasul, G., Q. Z. Chaudhry, A. Mahmood, K. W. Hyder and Q. Dahe, 2011: Glaciers and Glacial Lakes under Changing Climate in Pakistan. Pakistan Journal Of meteorology, 8(15) 1-8

Shrestha, M., L. Wang, T. Koike, Y. Xue, and Y. Hirabayashi, 2010: Improving the snow physics of WEB-DHM and its point evaluation at the SnowMIP sites.Hydrology and Earth System Sciences 14, no. 12 (2010): 2577-2594.

Shrestha, M., W. Lei, T. Koike., X. Yongkang, and H. Yukiko, 2012: Modeling the spatial distribution of snow cover in the Dudhkoshi region of the Nepal Himalayas. Journal of Hydrometeorology, 13(1), 204-222.

Tahir, A. A., 2011: Modeling snowmelt-runoff under climate scenarios in the Hunza River basin, Karakoram Range, Northern Pakistan."Journal of Hydrology 409.1: 104-117.

Tarboton and G .David. 1997: A new method for the determination of flow directions and upslope areas in grid digital elevation models. *Water resources research, 33*(2), 309-319.

Thenkabail, S. Prasad, M. Schull, and H. Turral 2005: Ganges and Indus river basin land use/land cover (LULC) and irrigated area mapping using continuous streams of MODIS data." Remote Sensing of Environment 95.3: 317-341.

Verdin, L .Kristine and P .James, 1999: A topological system for delineation and codification of the Earth’s river basins. *Journal of Hydrology, 218*(1), 1-12.

Wang, L., T. Koike, K. Yang, and P. J. FYeh, 2009: Assessment of a distributed biosphere hydrological model against stream flow and MODIS land surface temperature in the upper Tone River Basin, J. Hydrol., 377, 21–34, 2009b.

Wang, L., T. Koike, K. Yang, T. Jackson, R. Bindlish and D. Yang, 2009: Development of a distributed biosphere hydrological model and its evaluation with the Southern Great Plains Experiments (SGP97 and SGP99), J. Geophys. Res., 114, D08107, doi: 10.1029/2008JD010800, 2009a.

http://reverb.echo.nasa.gov /

https://rda.ucar.edu/datasets/ds628.0